

# Feasibility and safety of Taipei Veterans General Hospital Heavy Ion Therapy Center: The first carbon-ion irradiation facility in Taiwan

Tien-Li Lan<sup>a,b</sup>, Cheng-Ying Shiau<sup>a</sup>, Ling-Wei Wang<sup>a,b</sup>, Yu-Ming Liu<sup>a,b</sup>, Yi-Wei Chen<sup>a,b,c,d</sup>, Pin-I Huang<sup>a,b</sup>, Yu-Wen Hu<sup>a,b</sup>, I-Chun Lai<sup>a,b</sup>, Yuan-Hung Wu<sup>a,b</sup>, Tzu-Yu Lai<sup>a,b</sup>, Yu-Mei Kang<sup>a,b</sup>, Wan-Chin Yang<sup>a,b</sup>, Yu-Jung Lin<sup>a</sup>, Yi-Ying Pan<sup>a</sup>, Chi-Chuan Chiu<sup>a</sup>, Ching-Sheng Liu<sup>a</sup>, Tung-Sheng Hsieh<sup>a</sup>, Jia-Cheng Lee<sup>a,c</sup>, Fang-Yi Lin<sup>a</sup>, Chien-Hsuan Chan<sup>a</sup>, Hui-Chia Lin<sup>a</sup>, Keng-Li Lan<sup>a,e,\*</sup>

<sup>a</sup>Department of Heavy Particles and Radiation Oncology, Taipei Veterans General Hospital, Taipei, Taiwan, ROC; <sup>b</sup>School of Medicine, National Yang Ming Chiao Tung University, Taipei, Taiwan, ROC; <sup>c</sup>Department of Medical Imaging and Radiological Technology, Yuanpei University of Medical Technology, Hsinchu, Taiwan, ROC; <sup>d</sup>College of Nuclear Science, National Tsing-Hua University, Hsinchu, Taiwan, ROC; <sup>e</sup>Institute of Traditional Medicine, School of Medicine, National Yang Ming Chiao Tung University, Taipei, Taiwan, ROC

## Abstract

**Background:** Unlike conventional photon radiotherapy, particle therapy has the advantage of dose distribution. Carbon-ion radiotherapy is also advantageous in terms of biological effectiveness and other radiobiological aspects. These benefits lead to a higher response probability for previously known radioresistant tumor types. Therefore, Taipei Veterans General Hospital, which is located in the northern district of Taipei, built the first carbon-ion irradiation facility in Taiwan.

**Methods:** Taipei Veterans General Hospital completed a phase 1 trial to evaluate the safety of carbon-ion radiotherapy. Six patients (4 males and 2 females with prostate adenocarcinoma, sacral chordoma, hepatocellular carcinoma, lung adenocarcinoma, or parotid high-grade carcinoma) were enrolled in this study. The mean age of the patients was 62.7 years. The mean dose was 57.3 Gy(RBE) (fraction range, 4-16 Gy[RBE]).

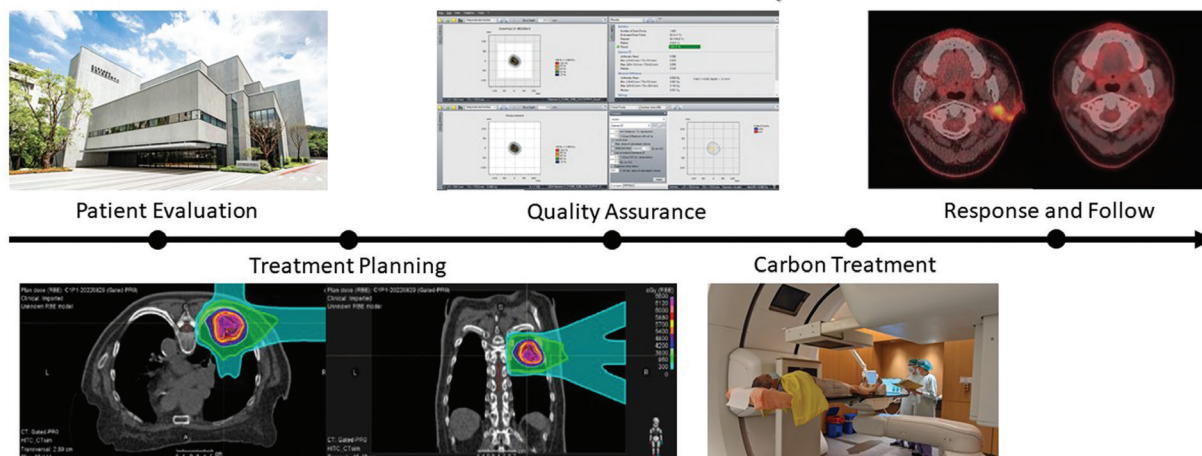
**Results:** During this phase 1 trial, all patients were monitored for 3 months to evaluate acute toxicity and short-term outcomes after treatment with carbon irradiation. Only 2 patients experienced grade 2 toxicity, which resolved without medication 1 month after completing treatment. The tumor response demonstrated 1 complete response, 1 partial response, and 4 cases of stable disease.

**Conclusion:** Carbon-ion radiotherapy was determined to be an effective and safe treatment.

**Keywords:** Carbon-ion radiotherapy; Outcomes; Toxicity; Tumor response

## Graphical abstract

### Feasibility and Safety of Taipei Veterans General Hospital Heavy Ion Therapy Center The first carbon-ion irradiation facility in Taiwan



Phase 1 Study to evaluate the Feasibility and Safety of the First Carbon-ion irradiation facility in Taiwan

- 2 Prostate cancers, 1 Sacrum sarcoma, 1 Liver HCC, 1 Lung adenocarcinoma, 1 Parotid gland tumor
- 1 Complete response, 1 Partial response, 4 Stable diseases
- 1 Grade 2 UTI, 1 Grade 2 pain, others denied treatment related discomfort

Lan TL et al. | Journal of the Chinese Medical Association (JCMA) 2025;88(3).

## 1. INTRODUCTION

Particle therapy has gained popularity in the field of radiation oncology. Theoretically, particle therapy has the potential to achieve better dose distribution compared with conventional external beam radiotherapy due to its physical properties.<sup>1,2</sup> The advantage of particle therapy is the Bragg peak, a physical phenomenon mainly related to Coulomb interactions that cause the particles to deliver their energy mainly at the end of the travel range.<sup>3</sup> Using this dose–depth relationship, we were able to create a plan to deliver particularly high doses while limiting the dose absorbed by nearby organs. Currently, the most popular clinically used particle therapies include proton and carbon therapies. Carbon-ion radiotherapy (CIRT) has higher relative biological effectiveness (RBE), a lower oxygen-enhancing ratio, and is capable of causing more DNA double-strand breaks, indicating a more lethal effect and better tumoricidal activity.<sup>4,5</sup> For some radioresistant tumor types, CIRT also has the potential to eliminate tumor cells because of its ability to cause damage. CIRT has been proven to have survival benefits and better tumor control than conventional radiotherapy for pancreatic cancer,<sup>6,7</sup> sarcomas,<sup>8,9</sup> hepatocellular carcinoma,<sup>10,11</sup> salivary gland tumors,<sup>12,13</sup> and other malignancies.<sup>14,15</sup>

Taipei Veterans General Hospital built the first carbon-ion irradiation facility in Taiwan. Two treatment rooms were constructed for clinical treatment. Accelerator commissioning and beam quality assurance in the first treatment room were completed in July 2022. A phase 1 clinical trial was designed to confirm the safety of CIRT and observe any acute adverse events and early responses of the patients.

## 2. METHODS

### 2.1. Study criteria and follow-up

This prospective, single-arm, single-institute, phase 1 trial was performed to demonstrate the safety of CIRT at Taipei Veterans General Hospital. It was conducted in accordance with the guidelines of the Declaration of Helsinki and approved by the Institutional Review Board of Taipei Veterans General Hospital (approval number: 0400TC02-2021-02-013C: S001-006), which was approved on December 3, 2021. We enrolled six patients with at least three different types of malignancies, including head and neck cancers, lung cancer, hepatobiliary carcinoma, prostate cancer, and bone or soft tissue sarcomas. All patients were required to undergo computed tomography imaging, magnetic resonance imaging (MRI), or positron emission tomography (PET) imaging before CIRT and imaging using the same modality at 12 weeks after CIRT. The inclusion criteria were as follows: age 20 years or older; tumor size smaller than 12 cm; no evidence of distant metastasis; life expectancy of 12 weeks or more; Eastern Cooperative Oncology Group performance status of 0 to 2; able to participate in the entire treatment procedure; and agreed to undergo CIRT after providing written informed consent. The exclusion criteria were as

follows: body weight of 135 kg or more; previous irradiation of the same area as that receiving CIRT; other malignancies that were not controlled or currently undergoing treatment; other local treatments that might interfere with the evaluation of the effectiveness of CIRT within 4 weeks before enrollment; and participation in other clinical trials within 12 weeks. No concurrent chemotherapy or immunotherapy was administered during the treatment period. Patients with other contraindications for CIRT, such as pacemaker use or the use of other internal electronic devices, were also excluded.

### 2.2. Treatment planning system and biological model

The treatment planning system used for calculating carbon-ion treatment is conducted by VQA Plan. A modified microdosimetric kinetic model (MKM model) is adopted to calculate RBE, defining the ratio to convert physical dose into the prescribed clinical dose. For critical organ constraints, we adhere to the experience of the Japan Carbon-ion Radiation Oncology Study Group (JCROS). Specifically, for the rectum, the constraints entail receiving less than 9.2 cc at 50% of the prescribed dose ( $V_{50\%}$ ), less than 6.2 cc at 70% ( $V_{70\%}$ ), less than 4.5 cc at 80% ( $V_{80\%}$ ), less than 2.5 cc at 90% ( $V_{90\%}$ ), and no part receiving  $V_{100\%}$ . In addition, other constraints are integrated into the treatment planning system for inverse planning.

### 2.3. Treatment information and management of breathing

The CIRT facility at Taipei Veterans General Hospital uses scanning beam irradiation, using both horizontal and vertical beams. Couch rotation in the roll and yaw directions is available, with a maximum of 10° allowed when planning noncoplanar irradiation. To manage patient breathing and mitigate potential interplay effects, the Anzai respiratory gating system is used to minimize breathing-related dose uncertainty. A 3 mm movement threshold in each direction is deemed acceptable, determining the breathing phases for irradiation.

### 2.4. Patient quality assurance

All CIRT treatment plans were evaluated using patient-specific quality assurance procedures, including two-dimensional dose distribution configuration verification. The treatment plans were deemed acceptable when the passing rate was 90% with a distance to agreement of 3 mm and a dose difference of 3%.<sup>16</sup>

### 2.5. Evaluation of the treatment response and adverse events

The response criteria were based on the Response Evaluation Criteria in Solid Tumors version 1.1. A complete response comprised the disappearance of all lesions. A partial response comprised a decrease in the longest diameter of the tumor by 30% or more. Progressive disease comprised an increase in the longest diameter of the tumor by 20% or more or the appearance of new lesions. Stable disease comprised none of these factors.<sup>17</sup> Acute adverse events were based on the Common Terminology Criteria for Adverse Events version 4.03. These were evaluated during treatment and at least 12 weeks after the completion of CIRT. Treatment was discontinued if the patient experienced intolerable acute treatment-related toxicity.<sup>18</sup>

### 2.6. Patient characteristics and doses

The baseline characteristics of all patients are summarized in Table 1, and the individual patient characteristics and CIRT doses are listed in Table 2.

\*Address correspondence: Dr. Keng-Li Lan, Department of Heavy Particles and Radiation Oncology, Taipei Veterans General Hospital, 201 Section 2, Shi-Pai Road, Taipei 112, Taiwan, ROC. E-mail address: kllan@vghtpe.gov.tw (K.-L. Lan).

Conflicts of interest: The authors declare that they have no conflicts of interest related to the subject matter or materials discussed in this article.

Journal of Chinese Medical Association. (2025) 88: 196-204.

Received March 24, 2023; accepted August 1, 2024.

doi: 10.1097/JCMA.0000000000001207

Copyright © 2025, the Chinese Medical Association. This is an open access article under the CC BY-NC-ND license (<http://creativecommons.org/licenses/by-nc-nd/4.0/>)

**Table 1****Baseline characteristics of all patients**

	All patients
Age, y	62.7 (range, 40-79)
Sex, M and F	4 and 2
Dose, Gy(RBE)	57.3 (range, 51.6-64)
BED <sub>10</sub> , Gy(RBE)	99.88 (range, 73.79-150)
Fractions	10.7 (range, 4-16)

BED<sub>10</sub> = biological effective dose ( $\alpha/\beta = 10$ ); F = female; Gy(RBE) = Gray equivalent; M = male.

**2.6.1. Patient 1**

Patient 1 was a 64-year-old man with prostate adenocarcinoma (cT2aN0M0), a Gleason score of 3 + 3, and no observed distant metastasis during the staging workup. After a multidisciplinary discussion, the patient was enrolled in our study. The clinical target volume (CTV) was 51.6 Gy(RBE) in 12 fractions to the entire prostate and proximal 1 cm of the seminal vesicle. Two lateral fields with each delivering 4.3 Gy(RBE) were designed (Fig. 1). The irradiation direction was switched daily, and the treatment was performed 4 days per week. The planning target volume (PTV) was an 8-mm lateral margin that was 5 mm from other margins. The patient was immobilized with a plastic pelvic shell and placed in the supine position. The treatment started on June 3, 2022. It ended successfully on July 19, 2022.

**2.6.2. Patient 2**

Patient 2 was a man with prostate adenocarcinoma (cT2bN0M0), a Gleason score of 3 + 4, and no evidence of distant metastasis. The CTV, PTV definition, treatment position, dose prescription, and fraction size were the same as those used for patient 1. After seven treatment fractions, variation in the body shape was observed; this impaired the immobilization ability of the pelvic shell. Therefore, we remodeled the pelvic shell and modified the treatment plan using deformed registration to establish the new dose distribution based on the previously irradiated area. The patient started treatment on July 25, 2022. Treatment was halted from August 5, 2022, to August 10, 2022, because of an accelerator malfunction. Treatment was completed on August 17, 2022.

**2.6.3. Patient 3**

Patient 3 was a 60-year-old man with sacral chordoma. The MRI evaluation on June 18, 2022, revealed a 108- × 85- × 92-mm heterogeneous lesion (cT4aN0) with contrast enhancement over the sacrum. Further imaging showed no evidence of distant metastasis. We imported the MRI and performed image fusion using simulation computed tomography. The CTV was contoured along the margin of the gross tumor, and the PTV was 5 mm in all directions. The prescribed dose was 64 Gy(RBE)

in 16 fractions with the patient in the prone position using a belly board to reduce the dose to the intestine and bladder. The irradiation field was divided into three directions (one vertical and two horizontal beams). Irradiation included 2.67 Gy(RBE) from the vertical beam for every fraction and 1.33 Gy(RBE) from the horizontal beam alternating from the left side to the right side daily (Fig. 2). Therefore, the target received 4 Gy(RBE) every day, and the repair time for the irradiated normal organs was increased. The patient started treatment on July 26, 2022. Treatment was halted from August 5, 2022, to August 10, 2022, because of an accelerator malfunction. Treatment was completed on August 23, 2022.

**2.6.4. Patient 4**

Patient 4 was a 72-year-old man with hepatocellular carcinoma (cT1bN0) and Barcelona clinic liver cancer stage A. He had a medical history of hepatitis B and liver cirrhosis that were regularly followed up and favorably controlled. The imaging study showed a 2.5- × 2.3-cm lesion over the right hepatic lobe with early arterial enhancement and early wash-out, which indicated hepatocellular carcinoma. No evidence of distant metastasis was noted. Because the patient refused radiofrequency ablation and surgery, he was enrolled in the CIRT trial. The patient was immobilized using a body cast. The Anzai respiratory system was used to evaluate the tumor position compared to the surface during each breathing phase. The respiratory threshold was regulated at a relative respiratory level of 10%, which represented a respiratory phase of approximately 50 to 70. The gross tumor volume (GTV) was delineated by fusing the diagnostic MRI with the computed tomography simulation image; a margin of 5 mm was added to define the CTV. To create the internal target volume, the PTV was further enlarged by adding a margin 3 mm from the CTV because of the internal respiratory motion indicated by the Anzai respiratory system. The total dose was 52.8 Gy(RBE) in four fractions. Hypofractionated treatment is suitable for the peripheral tumor and is delivered at a safe distance from the duodenum and intestine. The field was designed using three different directions (vertical beam, horizontal beam without couch rotation, and horizontal beam with 15° yaw rotation of the couch) (Fig. 3). Each of the beams delivered a daily fraction of 4.4 Gy(RBE), and the entire treatment interval was completed within 1 week. Treatment was started on August 25, 2022. It ended on August 30, 2022.

**2.6.5. Patient 5**

Patient 5 was a 79-year-old woman with lung cancer. Her biopsy results revealed adenocarcinoma. Computed tomography showed a 2.1-cm lesion with clinical stage T1cN0M0 over the right lower lobe without mediastinal lymphadenopathy or distant metastasis. After a multidisciplinary discussion, it was determined that surgery or CIRT was indicated for local tumor control. After a thorough discussion with the patient,

**Table 2****Individual patient characteristics and CIRT doses**

	Patient 1	Patient 2	Patient 3	Patient 4	Patient 5	Patient 6
Age, sex	64, M	61, M	60, M	72, M	79, F	40, F
Diagnosis	Prostate adenoCA	Prostate adenoCA	Sacrum chordoma	Liver HCC	Lung adenoCA	Parotid gland high-grade CA
Clinical staging	T2aNOMO	T2bNOMO	T4aNOMO	T1bNOMO	T1cNOMO	T4aNOMO
Dose, Gy(RBE)	51.6	51.6	64	52.8	60	64
Fractions	12	12	16	4	4	16

adenoCA = adenocarcinoma; CA = carcinoma; CIRT = carbon-ion radiotherapy; F = female; Gy(RBE) = Gray equivalent; HCC = hepatocellular carcinoma; M = male.

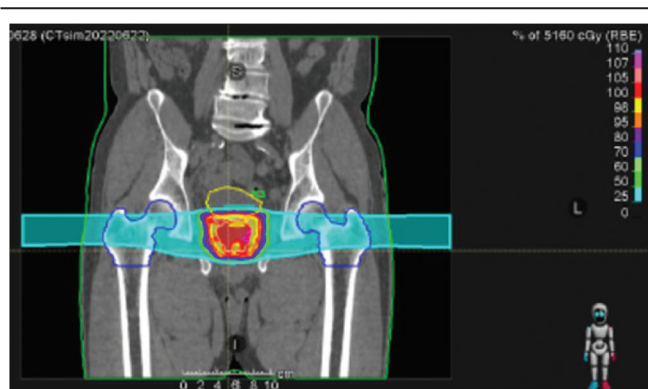


Fig. 1 Dose distribution for patient 1.

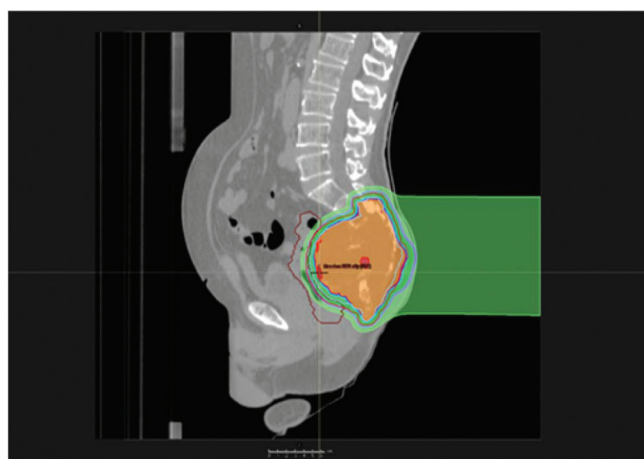


Fig. 2 Dose distribution for patient 3. The patient was immobilized in the prone position with a belly board to minimize the dose to the intestine and bladder.

she decided to undergo CIRT. The patient was immobilized and treated in the prone position. The Anzai respiratory gating system was used to track the target and minimize the radiation dose to the normal lung and adjacent normal organs. The respiratory threshold was designated based on the tumor internal motion of 3 mm in each direction, resulting in a final gating level of 20%, which was converted to a respiratory phase of 30 to 70. The total dose for this patient was 60 Gy(RBE) in four daily fractions. Every 15-Gy(RBE) fraction was further divided into the following four directions: 3.75 Gy(RBE) in the vertical field and

3.75 Gy(RBE) in three horizontal fields (one with no couch rotation, one with yaw rotation of 20°, and one with yaw rotation of 340°) (Fig. 4). CIRT was started on September 1, 2022. It was completed on September 6, 2022.

#### 2.6.6. Patient 6

Patient 6 was a 40-year-old woman with high-grade parotid gland carcinoma. MRI and PET revealed a mass lesion (cT4aN0M0) in the left parotid gland with ill-defined margins protruding into the left stylomastoid foramen and borderline regional lymphadenopathy at the same level of the primary tumor over level 2a. The biopsy results showed poorly differentiated carcinoma. The neurologic examination showed no neurologic deficits. Surgery was not indicated because of the probability of facial nerve involvement. Therefore, she enrolled in this CIRT trial. She was immobilized using a thermoplastic mask with her neck rotated to the right side to avoid the vertical beam passing through the mandible, which could have created unnecessary dose uncertainty. The GTV was contoured based on the MRI and PET images including the parotid gland tumor and lymphadenopathy over cervical level 2a. Treatment was divided into two phases. During the first phase, the CTV1 was defined as the GTV plus the entire parotid gland and adjacent lymphatic drainage. A 2-mm outer margin was added to create the PTV1, and 36 Gy(RBE) was delivered in nine fractions. The patient underwent a second computed tomography simulation to allow for replanning. During the second phase, the CTV2 was defined by narrowing the range to the GTV with a 5-mm outer margin to allow focal boost. An additional 28 Gy(RBE) in seven fractions was prescribed for the PTV2, which was created by adding an outer margin of 2 mm from the CTV2 (Fig. 5). The entire procedure comprised a total of 16 fractions and lasted from September 7, 2022, to September 30, 2022.

### 3. RESULTS

During this phase 1 trial, all patients were followed up for 3 months to evaluate acute toxicities after treatment with CIRT. The tumor response was also assessed. However, the actual control probability requires longer follow-up because previous CIRT studies demonstrated that tumor shrinkage in some cases requires more time than that achieved with conventional radiotherapy.<sup>19,20</sup> The overall treatment response of each patient is listed in Table 3.

No adverse events were noted for patients 1 and 2, who were both diagnosed with prostate adenocarcinoma and treated with 51.6 Gy(RBE) in 12 fractions. Based on the MRI, both patients had stable disease. Regarding the prostate-specific

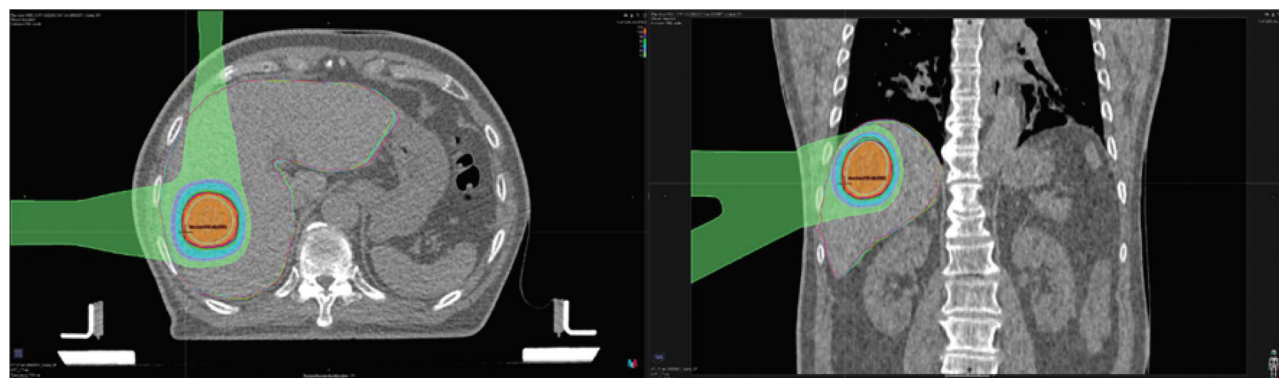
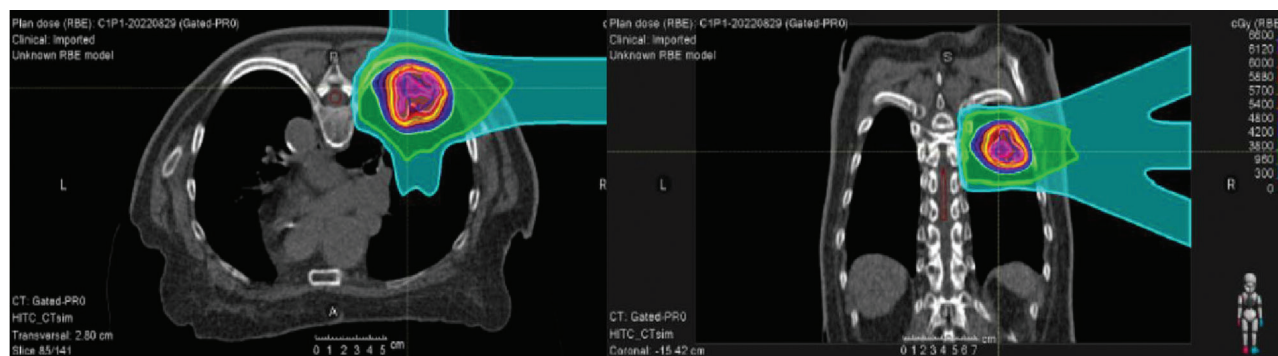
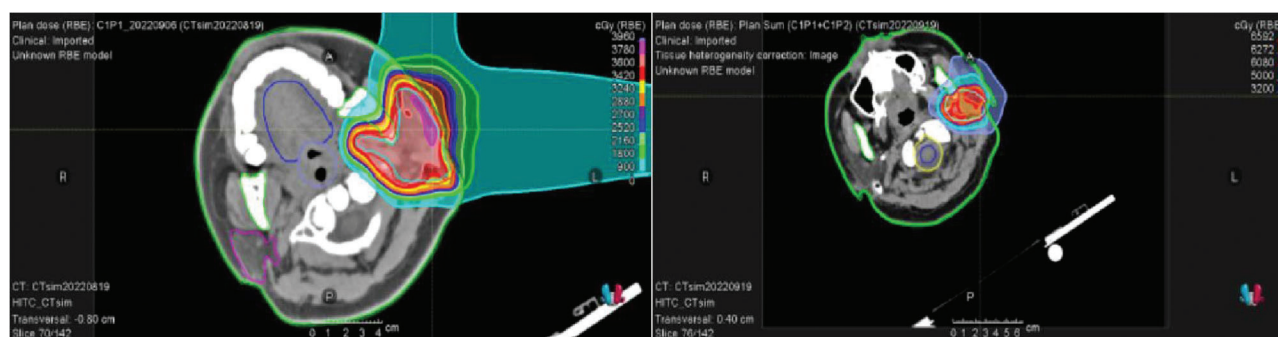


Fig. 3 Dose distribution for patient 4. The axial view (left) and coronal view (right) show the three irradiation directions.



**Fig. 4** Dose distribution for patient 5. The patient was treated in the prone position. The axial view (left) and coronal view (right) show the beam directions: one from the vertical beam and three from different directions from the horizontal beam using couch rotation.



**Fig. 5** Dose distribution for patient 6. Left, The beam direction with the patient immobilized by a thermoplastic mask and the neck rotated to the right side to decrease dose uncertainty. Right, The summed dose distribution of two treatment phases with the tumor and lymphadenopathies boosted for seven fractions.

**Table 3**

**Treatment response according to the RECIST criteria and acute adverse events based on CTCAE version 4.03**

	Treatment response (RECIST)	Adverse events (CTCAE)
Patient 1	SD	-
Patient 2	SD	-
Patient 3	SD with regression of contrast enhancement	Grade 2 UTI, grade 2 RD
Patient 4	CR	-
Patient 5	SD	-
Patient 6	PR with faint uptake indicated by PET imaging	Grade 2 pain, grade 1 RD

- = no adverse event noticed; CR = complete response; CTCAE = Common Terminology Criteria for Adverse Events; PERCIST = PET response criteria in solid tumors; PET = positron emission tomography; PMR = partial metabolic response; PR = partial response; RD = radiation dermatitis; RECIST = Response Evaluation Criteria in Solid Tumors; SD = stable disease; UTI = urinary tract infection.

antigen (PSA) level, patient 1 experienced a slight increase from 1.12 ng/mL before treatment to 1.75 ng/mL after treatment, while patient 2 experienced a significant decrease from 5.18 ng/mL before treatment to 0.14 ng/mL at treatment completion.

Patient 3 with sacral chordoma received a total dose of 64 Gy(RBE) in 16 fractions. A grade 2 urinary tract infection was observed after treatment completion, but it was not related to CIRT. The infection was controlled with antibiotic administration. Grade 2 radiation dermatitis and symptoms of xeroderma were observed immediately after treatment; these symptoms improved without any medication at 1 month after CIRT completion. Regarding the treatment response, the MRI before CIRT showed a measurement of 110 × 95 × 110 mm; however, that after CIRT showed a measurement of 128 × 99 × 114 mm. According to the Response Evaluation Criteria in Solid Tumors version 4.03 criteria, stable disease was considered. However,

a slight increase in the tumor volume was regarded as tumor and tissue swelling after treatment, and an important finding of contrast enhancement regression was also observed (Fig. 6). Therefore, tumor shrinkage can be expected because most components of the tumor mass may be considered necrotic tissue.

Patient 4, who was diagnosed with hepatocellular carcinoma, was treated with CIRT using 52.8 Gy(RBE) in four fractions. The total bilirubin level increased from 1.04 to 1.37 mg/dL after treatment, which is 1.14 times the upper limit of normal (1.2 mg/dL). The patient did not report any discomfort during treatment. An imaging study performed 3 months after CIRT demonstrated a complete response of the liver tumor (Fig. 7). The high-signal area without arterial phase enhancement over S8 of the liver observed during the T2 phase of MRI was considered a CIRT-related change by radiology experts.

Patient 5, who was diagnosed with lung cancer, was treated with CIRT using 60 Gy(RBE) in four fractions. No adverse events were observed during or after CIRT. Computed tomography performed 3 months after CIRT completion showed no interval change in the size of the right lower lung lesion. No obvious radiation-related lung damage was observed during the imaging study.

Patient 6 presented with high-grade carcinoma of the parotid gland, along with a swollen lymph node that did not show uptake on PET imaging at the cervical lymphatic level 2a. This patient underwent CIRT in two phases with 36 Gy(RBE) in nine fractions to the entire parotid gland and adjacent lymphatic drainage and a boost to a total of 64 Gy(RBE) in 16 fractions to the gross tumor. This patient experienced grade 1 radiation dermatitis during treatment and grade 2 pain over the irradiated area, which were relieved with medication. Surprisingly, no oral or pharyngeal mucositis was observed during or after treatment; these are common adverse events with conventional

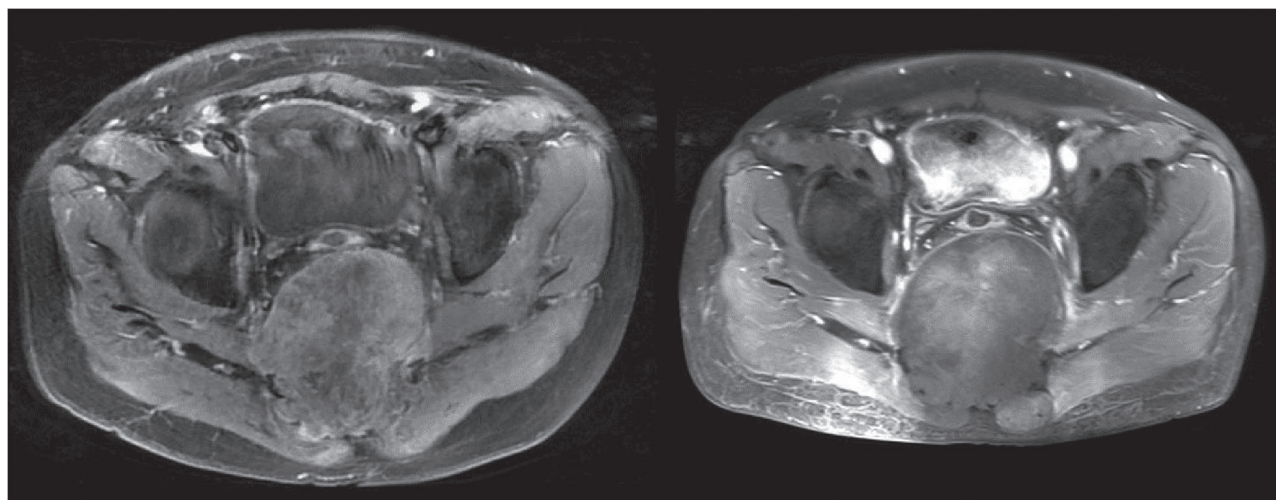


**Fig. 6** Magnetic resonance images before CIRT (left) and 3 mo after CIRT (right) of patient 3. The tumor size showed no obvious shrinkage; however, decreased contrast enhancement was noticed, which might indicate necrotic changes of the tumor mass. CIRT = carbon-ion radiotherapy.

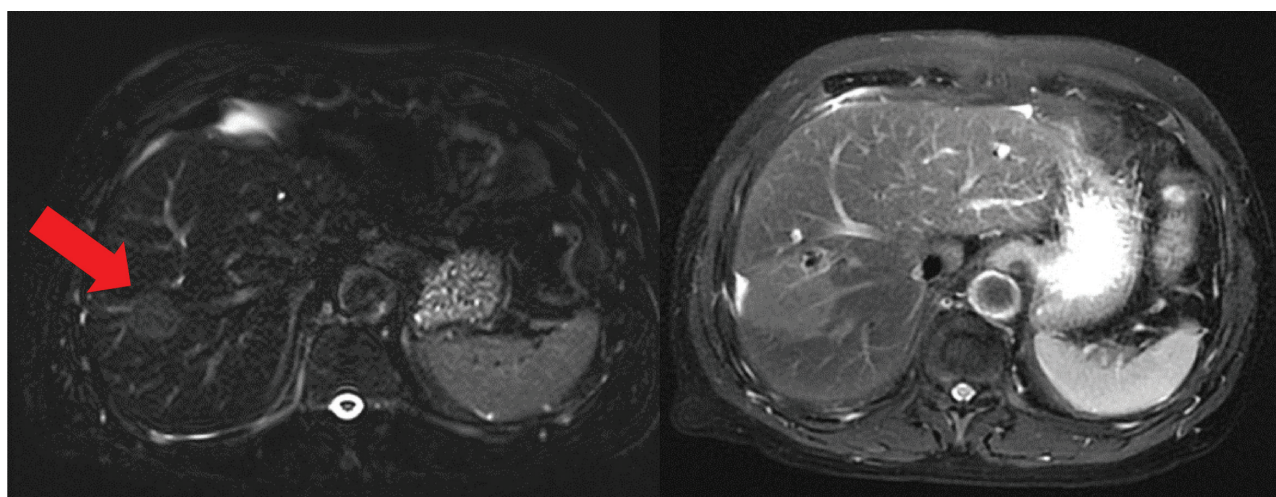


**Fig. 7** Magnetic resonance images before CIRT (left) and 3 mo after CIRT (right) of patient 4. The red arrow shows the tumor with early enhancement in the arterial phase. After CIRT, the tumor completely disappeared. The radiation effect (right) appears as a high-signal area in the T2 phase. CIRT = carbon-ion radiotherapy.

radiotherapy. The patient tolerated the entire CIRT duration without a treatment break. MRI and PET at 3 months after CIRT showed a partial response, a significant decrease in fluorodeoxyglucose uptake over the left parotid lesion, and disappearance of the previously noted neck lymphadenopathies (Fig. 8).

#### 4. DISCUSSION

This phase 1 trial was designed to confirm the safety of this new treatment modality performed at the first carbon-ion irradiation facility in Taiwan. Because of the large amount of global clinical evidence of the benefits of CIRT, we were able to operate our system after the beam quality was confirmed and adverse effects were controlled. The patient selection criteria were based on the consensus of the radiation oncologists of the Taipei Veterans General Hospital Radiation Oncology Department. The dose prescriptions and dose constraints for normal organs were determined previously.<sup>19,20</sup>

The optimal dose of CIRT for prostate cancer remains controversial.<sup>21</sup> Currently, many CIRT facilities use a dose of 51.6

Gy(RBE) in 12 fractions to treat prostate cancer.<sup>22</sup> However, a retrospective study showed that 66 Gy(RBE) in 20 fractions is significantly preferable to 51.6 Gy(RBE) in 12 fractions because of its biochemical failure-free rate.<sup>23</sup> The initial design of the moderately hypofractionated regimen in 12 fractions was determined according to the biologically effective dose transformation using the estimated  $\alpha/\beta$  value of 1.5 for prostate adenocarcinoma; however, the clinical RBE might decrease as the fraction size increases, causing an underestimation of the suitable dose in 12 fractions. Recently, a new dose regimen comprising 60 Gy(RBE) in four fractions was proposed by the JCROS based on this important finding after considering the RBE. The results will be published in the near future.

Another important finding of previous studies is the event of a PSA bounce.<sup>24,25</sup> Many patients who received CIRT experienced an increased PSA level immediately after treatment, followed by a gradual decrease to a normal PSA level (<0.2 ng/mL).<sup>26</sup> These studies showed a significantly better biochemical failure-free rate for patients who exhibited a PSA bounce. In our cohort, patient 1 experienced a slight increase in the PSA level after

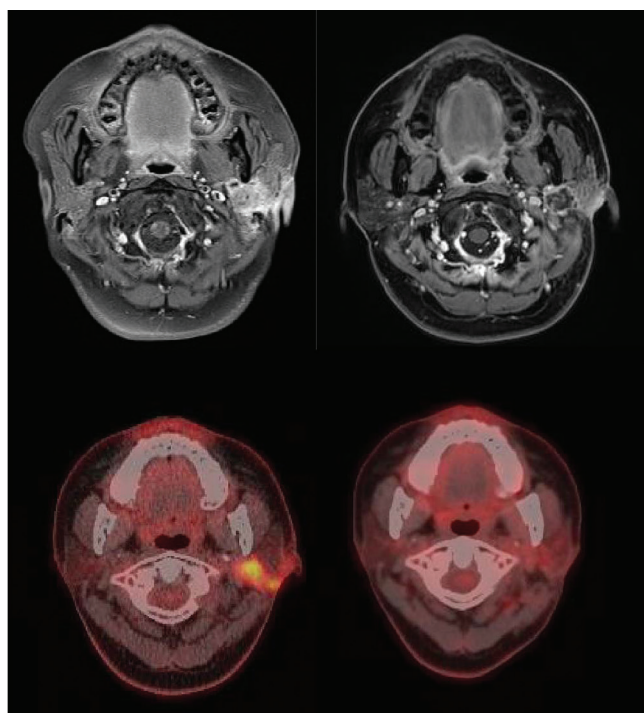


**Fig. 8.** Imaging studies of patient 6. MRI before CIRT (left upper panel). PET image before CIRT (left lower panel). MRI 3 mo after CIRT. The left parotid lesion has a decreased size and reduced contrast enhancement (right upper panel). PET image 3 mo after CIRT. Significantly reduced fluorodeoxyglucose uptake was noticed (right lower panel). CIRT = carbon-ion radiotherapy; MRI = magnetic resonance imaging; PET = positron emission tomography.

CIRT. However, this patient received anti-hormone medications after CIRT for tumor control, which might have affected the factuality of the PSA level compared with that with CIRT alone. For patients with prostate cancer at an unfavorable intermediate risk level or above, we will prescribe antihormone medications for 2 months before commencing carbon-ion therapy. This may render the evaluation of treatment response via PSA levels more unreliable. Hence, for these patients, we recommend continuing anti-hormone medications for 6 months and monitoring PSA levels every 3 months post-treatment. We anticipate a gradual decrease in PSA levels, which should stabilize once the treatment-related inflammatory processes have subsided.

Many studies have shown the importance of considering the water equivalent distance of the beam pathway when planning CIRT and the management of potential setup errors caused by daily setup deviations or internal organ motion. Adding a beam-specific PTV to manage errors when matching the tumor in the treatment field and avoid nearby diverged organs has been beneficial.<sup>27</sup> This phenomenon is particularly important when we use fiducial markers to match the target site because the relative positions of the tumors and normal organs might be ignored, thus causing the particle beam to be attenuated at a different scale as the media density changes.<sup>28,29</sup> For example, to reduce the dose to the bladder and rectum when treating prostate cancer, we used bilateral irradiation, which involves the beam traveling through the fat, muscles, and femoral head. When a patient has a random event with a different bladder volume or lack of bowel preparation, the position of the prostate might also change. This results in a change in the bony structure through which the beam travels if the center of the beam is still targeting the prostate. If a shorter water equivalent length is traveled, then this might cause an underdose to the proximal side of the

target and an overdose to the organs on the distal side of the target. With conventional photon radiotherapy, this effect has less impact on the dose distribution because intensity-modulated radiation therapy and volumetric-modulated arc therapy usually focus on the irradiation target in the center of the field and use different angles to accumulate the dose in the target volume. To address this problem, we usually add a beam-specific PTV.<sup>30</sup> However, adding the beam-specific PTV might result in a less preferred dose distribution, thus causing more spillage of the dosage to the nearby normal organs. This is also critical when treating lung cancer because the ribs shift with the respiratory cycle, thus causing changes in the irradiation field. In the future, we plan to apply treatment angles so the beam can pass high-density body parts as much as possible. Another strategy is the deep inspiration breath-hold, which can lessen the impact of rib movement on the change in the dose distribution.

With the virtual quality assurance treatment planning system, the modified MKM is integrated and considers the dose-dependent RBE in relation to the clinical dose.<sup>31-33</sup> Currently, there are several models in use. The most popular model in Europe is the local effect model,<sup>34</sup> and that in Japan is the Kanai model.<sup>35</sup> The diversity of models in use greatly affects the actual dose received by the target.<sup>36,37</sup> Further evaluation of the proper biological weighting models should be performed to convert and prescribe the sufficient carbon-ion dosage for the tumor.

At the Taipei Veterans General Hospital carbon-ion irradiation facility, we have two treatment rooms with fixed horizontal and vertical gantries. One of the treatment rooms includes an in-room computed tomography device as well. A drawback of our fixed gantry device is the lack of beam angles to approach the tumor while sparing the critical organs nearby. Even though CIRT and other particle therapies are well-known for their Bragg peak, which delivers most of its energy at a certain depth after passing the medium, the entry dose and fragmentation tail both accumulate a low dose, which may result in late complications in the future.<sup>38</sup> To compensate for this issue, we developed a few strategies to lower the probability of normal tissue complications. The first is tilting the treatment couch or adding a vacuum bag to rotate the patient position in relation to the beam direction. Using this method, we separated the daily fraction into two to four segments and effectively dispersed the doses received by the organs at risk. Based on our experience, yaw rotation does not cause any discomfort to the patient; however, there is a limitation of 10° in the pitch and roll rotation, which may lead to safety issues because the patient could fall off the treatment couch. To counteract this potential safety issue, we used a plastic body shield to protect the patient from falling. Unfortunately, shield deformation was observed when no other support was used for the patient's weight. Currently, we are evaluating different materials to strengthen the shield or design body casts using three-dimensional printing techniques. For patients 4 and 5, we designed a multiple-direction irradiation technique using yaw rotation, which could potentially reduce normal tissue damage based on the normal tissue compensation probability model.<sup>39</sup> The main deficits of this multifield method are the increased total treatment time and possible intrafractional organ motion. The actual benefits of this modality should be further analyzed by future studies.

As part of future research directions, the carbon-ion facility at Taipei Veterans General Hospital is actively investigating the variances in immune response between carbon-ion treatment and conventional external beam radiotherapy. In addition, efforts are underway to explore new indications for carbon-ion therapy, such as pelvic irradiation for prostate cancer patients at high risk of lymph node metastasis. Through these endeavors, we aim to optimize the utilization of our facility and extend

the benefits of more precise and potent treatments to a greater number of cancer patients.

In conclusion, the Taipei Veterans General Hospital carbon-ion irradiation facility is the first of its kind in Taiwan. This phase 1 trial proved the safety of this facility. However, the treatment effects and those of conventional treatment require longer follow-up periods before they can be confirmed. We are considering how to possibly optimize these procedures. In the future, we hope to share our clinical experience and stay in close connection with carbon-ion facilities worldwide to confer benefits to cancer patients treated at Taipei Veterans General Hospital.

## ACKNOWLEDGMENTS

The authors thank Hitachi Heavy Industry for partial funding for the CIRT treatment. The authors thank Qualtech Consulting Corporation for making this clinical trial proceed smoothly.

## REFERENCES

- Palm A, Johansson KA. A review of the impact of photon and proton external beam radiotherapy treatment modalities on the dose distribution in field and out-of-field; implications for the long-term morbidity of cancer survivors. *Acta Oncol* 2007;46:462–73.
- Mohan RA. Review of proton therapy—current status and future directions. *Precis Radiat Oncol* 2022;6:164–76.
- Sawakuchi GO, Titt U, Mirkovic D, Mohan R. Density heterogeneities and the influence of multiple Coulomb and nuclear scatterings on the Bragg peak distal edge of proton therapy beams. *Phys Med Biol* 2008;53:4605–19.
- Ming X, Wang W, Shahnazi K, Sun J, Zhang Q, Li P, et al. Dosimetric comparison between carbon, proton and photon radiation for renal retroperitoneal soft tissue sarcoma recurrence or metastasis after radical nephrectomy. *Int J Radiat Biol* 2022;98:183–90.
- Fujii O, Demizu Y, Hashimoto N, Araya M, Takagi M, Terashima K, et al. A retrospective comparison of proton therapy and carbon ion therapy for stage I non-small cell lung cancer. *Radiother Oncol* 2013;109:32–7.
- Hagiwara Y, Yamada S, Isozaki Y, Takiyama H, Shinoto M, Kawashiro S, et al. Efficacy and feasibility of re-irradiation using carbon ions for pancreatic cancer that recurs after carbon-ion radiotherapy. *Clin Transl Radiat Oncol* 2021;26:24–9.
- Shinoto M, Terashima K, Suefuiji H, Matsunobu A, Toyama S, Fukunishi K, et al. A single institutional experience of combined carbon-ion radiotherapy and chemotherapy for unresectable locally advanced pancreatic cancer. *Radiother Oncol* 2018;129:333–9.
- Shiba S, Okamoto M, Kiyohara H, Okazaki S, Kaminuma T, Shibuya K, et al. Impact of carbon ion radiotherapy on inoperable bone sarcoma. *Cancers (Basel)* 2021;13:1099.
- Imai R, Kamada T, Araki N; Working Group for Carbon Ion Radiotherapy for Bone and Soft Tissue Sarcomas. Carbon ion radiotherapy for unresectable localized axial soft tissue sarcoma. *Cancer Med* 2018;7:4308–14.
- Shibuya K, Ohno T, Terashima K, Toyama S, Yasuda S, Tsuji H, et al; Japan Carbon Ion Radiotherapy Study Group. Short-course carbon-ion radiotherapy for hepatocellular carcinoma: a multi-institutional retrospective study. *Liver Int* 2018;38:2239–47.
- Habermehl D, Debus J, Ganten T, Ganten MK, Bauer J, Brecht IC, et al. Hypofractionated carbon ion therapy delivered with scanned ion beams for patients with hepatocellular carcinoma—feasibility and clinical response. *Radiat Oncol* 2013;8:59.
- Jensen AD, Poulakis M, Vanoni V, Uhl M, Chaudhri N, Federspil PA, et al. Carbon ion therapy (C12) for high-grade malignant salivary gland tumors (MSGTs) of the head and neck: do non-ACCs profit from dose escalation? *Radiat Oncol* 2016;11:90.
- Hayashi K, Koto M, Demizu Y, Saitoh JI, Suefuiji H, Okimoto T, et al; Japan Carbon-Ion Radiation Oncology Study Group. A retrospective multicenter study of carbon-ion radiotherapy for major salivary gland carcinomas: subanalysis of J-CROS 1402 HN. *Cancer Sci* 2018;109:1576–82.
- Schmid MP, Held T, Lang K, Herfarth K, Hörner-Rieber J, Harrabi SB, et al. Intensity modulated radiotherapy with carbon ion radiotherapy boost for acinic cell carcinoma of the salivary glands. *Cancers (Basel)* 2021;13:124.
- Saitoh JI, Koto M, Demizu Y, Suefuiji H, Ohno T, Tsuji H, et al; Japan Carbon-Ion Radiation Oncology Study Group. A multicenter study of carbon-ion radiation therapy for head and neck adenocarcinoma. *Int J Radiat Oncol Biol Phys* 2017;99:442–9.
- Mori S, Takei Y, Shirai T, Hara Y, Furukawa T, Inaniwa T, et al. Scanned carbon-ion beam therapy throughput over the first 7 years at National Institute of Radiological Sciences. *Phys Med* 2018;52:18–26.
- Schwartz LH, Litière S, de Vries E, Ford R, Gwyther S, Mandrekas S, et al. RECIST 1.1-Update and clarification: from the RECIST committee. *Eur J Cancer* 2016;62:132–7.
- Common Terminology Criteria for Adverse Events (CTCAE) version 4.03*. Bethesda, MD: National Cancer Institute; 2009. Revised 2010 June.
- Okada T, Kamada T, Tsuji H, Mizoe JE, Baba M, Kato S, et al. Carbon ion radiotherapy: clinical experiences at National Institute of Radiological Science (NIRS). *J Radiat Res* 2010;51:355–64.
- Kamada T, Tsujii H, Blakely EA, Debus J, De Neve W, Durante M, et al. Carbon ion radiotherapy in Japan: an assessment of 20 years of clinical experience. *Lancet Oncol* 2015;16:e93–100.
- Darwis NDM, Oike T, Kawamura H, Kawahara M, Kubo N, Sato H, et al. Kinetics of prostate-specific antigen after carbon ion radiotherapy for prostate cancer. *Cancers (Basel)* 2020;12:589.
- Ishikawa H, Tsuji H, Murayama S, Sugimoto M, Shinohara N, Maruyama S, et al. Particle therapy for prostate cancer: the past, present and future. *Int J Urol* 2019;26:971–9.
- Ishikawa H, Katoh H, Kaminuma T, Kawamura H, Ito K, Matsui H, et al; Group for Genitourinary Tumors at Gunma Heavy Ion Medical Center. Carbon-ion radiotherapy for prostate cancer: analysis of morbidities and change in health-related quality of life. *Anticancer Res* 2015;35:5559–66.
- Nomiya T, Tsuji H, Kawamura H, Ohno T, Toyama S, Shioyama Y, et al. A multi-institutional analysis of prospective studies of carbon ion radiotherapy for prostate cancer: a report from the Japan Carbon Ion Radiation Oncology Study Group (J-CROS). *Radiother Oncol* 2016;121:288–93.
- Kang YM, Ishikawa H, Inaniwa T, Iwai Y, Matsufuji N, Kasuya G, et al. The clinical relative biological effectiveness and prostate-specific antigen kinetics of carbon-ion radiotherapy in low-risk prostate cancer. *Cancer Med* 2023;12:1540–51.
- Yamamoto Y, Offord CP, Kimura G, Kuribayashi S, Takeda H, Tsuchiya S, et al. Tumour and immune cell dynamics explain the PSA bounce after prostate cancer brachytherapy. *Br J Cancer* 2016;115:195–202.
- Tsubouchi T, Hamatani N, Takashina M, Wakisaka Y, Ogawa A, Yagi M, et al. Carbon ion radiotherapy using fiducial markers for prostate cancer in Osaka HIMAK: treatment planning. *J Appl Clin Med Phys* 2021;22:242–51.
- Lin L, Kang M, Huang S, Mayer R, Thomas A, Solberg TD, et al. Beam-specific planning target volumes incorporating 4D CT for pencil beam scanning proton therapy of thoracic tumors. *J Appl Clin Med Phys* 2015;16:5678.
- Park PC, Zhu XR, Lee AK, Sahoo N, Melancon AD, Zhang L, et al. A beam-specific planning target volume (PTV) design for proton therapy to account for setup and range uncertainties. *Int J Radiat Oncol Biol Phys* 2012;82:e329–36.
- Liu W, Frank SJ, Li X, Li Y, Zhu RX, Mohan R. PTV-based IMPT optimization incorporating planning risk volumes vs robust optimization. *Med Phys* 2013;40:021709.
- Parisi A, Furutani KM, Beltran CJ. On the calculation of the relative biological effectiveness of ion radiation therapy using a biological weighting function, the microdosimetric kinetic model (MKM) and subsequent corrections (non-Poisson MKM and modified MKM). *Phys Med Biol* 2022;67:095014.
- Inaniwa T, Furukawa T, Kase Y, Matsufuji N, Toshito T, Matsumoto Y, et al. Treatment planning for a scanned carbon beam with a modified microdosimetric kinetic model. *Phys Med Biol* 2010;55:6721–37.
- Inaniwa T, Kanematsu N, Matsufuji N, Kanai T, Shirai T, Noda K, et al. Reformulation of a clinical-dose system for carbon-ion radiotherapy treatment planning at the National Institute of Radiological Sciences, Japan. *Phys Med Biol* 2015;60:3271–86.
- Grün R, Friedrich T, Elsässer T, Krämer M, Zink K, Karger CP, et al. Impact of enhancements in the local effect model (LEM) on the predicted

- RBE-weighted target dose distribution in carbon ion therapy. *Phys Med Biol* 2012;57:7261–74.
35. Fujitaka S, Fujii Y, Nihongi H, Nakayama S, Takashina M, Hamatani N, et al. Physical and biological beam modeling for carbon beam scanning at Osaka Heavy Ion Therapy Center. *J Appl Clin Med Phys* 2021;22:77–92.
  36. Grosshagauer S, Fossati P, Schafasand M, Carlino A, Poljanc K, Radakovits T, et al. Organs at risk dose constraints in carbon ion radiotherapy at MedAustron: Translations between LEM and MKM RBE models and preliminary clinical results. *Radiother Oncol* 2022;175:73–8.
  37. Zhang L, Wang W, Hu J, Lu J, Kong L. RBE-weighted dose conversions for patients with recurrent nasopharyngeal carcinoma receiving carbon-ion radiotherapy from the local effect model to the microdosimetric kinetic model. *Radiat Oncol* 2020;15:277.
  38. Buglewicz DJ, Walsh KD, Hirakawa H, Kitamura H, Fujimori A, Kato TA. Biological effects of monoenergetic carbon ions and their associated secondary particles. *Front Oncol* 2022;12:788293.
  39. Marks LB, Yorke ED, Jackson A, Ten Haken RK, Constine LS, Eisbruch A, et al. Use of normal tissue complication probability models in the clinic. *Int J Radiat Oncol Biol Phys* 2010;76(3Suppl):S10–9.